

## PARTON SATURATION EFFECTS TO THE DRELL-YAN PROCESS IN THE COLOR DIPOLE PICTURE

M.A. BETEMPS, M.B. GAY DUCATI, M.V.T. MACHADO

*Instituto de Fisica, Universidade Federal do Rio Grande do Sul,*

*Caixa Postal 15051, 91501-970, Porto Alegre, Brasil*

*E-mail: mandrebe@if.ufrgs.br, gay@if.ufrgs.br, magnus@if.ufrgs.br*

We report on the results obtained in the study of the parton saturation effects, taken into account through the multiscattering Glauber-Mueller approach, applied to the Drell-Yan (DY) process described in the color dipole picture. As a main result, one shows that those effects play an important role in the estimates of the DY differential cross section at RHIC energies.

The Drell-Yan (DY) process, i.e. the production of massive lepton pairs in hadronic collisions, in conjunction with deep inelastic scattering (DIS), has been one of the important processes probing strong interaction physics. Recently, in connection with the availability of high energy accelerators, a great attention has been focused on the small- $x$  region of QCD. There, the parton densities become high and the limits of the perturbative methods are tested. Such a region presents the onset of the saturation phenomenon (at scale  $Q_s^2$ ), i.e. the taming of the parton (mostly gluon) distribution due to nonlinear dynamics associated with unitarity effects<sup>1</sup>.

In this contribution, we study the high energy DY cross section in the target rest frame. In this case, the relevant degrees of freedom are the projectile wavefunction and the dipole-proton effective cross section. The underlying process is the scattering of a parton from the projectile structure function off the target color field. This parton radiates (bremsstrahlung) a massive photon, which subsequently decays into a lepton pair. The interaction with the target can occur before or after the photon emission. A remarkable feature emerging is that the  $\gamma^*q$ -proton (or hadron) interaction can be described by the same  $q\bar{q}$  (color dipole)-proton cross section as in DIS. Although diagrammatically no dipole is present, the interference among graphs results in a product of two quark amplitudes in the DY cross section testing the external gluonic field at two different transverse positions (impact parameters), in a similar way to DIS<sup>2</sup>.

In such a representation, the photoabsorption cross section on deep inelastic is described by the convolution of the wavefunctions,  $\Psi_{\gamma^*}$ , from the virtual photon and the interaction dipole cross section,  $\sigma_{dip}$ . The wavefunctions are considered taking into account the simplest photon Fock state configuration,

i.e., a  $q\bar{q}$ -pair fluctuation (dipole), whose transverse separation  $r_\perp$  remains fixed during the interaction since its lifetime is larger than the collision one. The  $\sigma_{dip}$  is modeled phenomenologically based on a matching between hard and soft domains, constrained by the DIS available data. Small dipole size configurations can be described through pQCD, whereas the large size ones belong to the nonperturbative domain. Hence, one can write the photoabsorptions cross section as a function of the Bjorken scaling variable  $\tilde{x} = x_{Bj}$ , the photon virtuality scale  $\tilde{Q}^2 = Q^2$  and the quark momentum fraction  $\alpha$  in the quantum mechanical form<sup>3</sup>,

$$\sigma_{T,L}(\gamma^* p \rightarrow q\bar{q}) = \int d^2 r_\perp \int_0^1 d\alpha |\Psi_{q\bar{q}}^{T,L}(\alpha, r_\perp, \tilde{Q}^2)|^2 \sigma_{dip}(\tilde{x}, r_\perp), \quad (1)$$

where the simplest phenomenological realization of the dipole cross section is given by the GBW model<sup>4</sup>,  $\sigma_{dip} = \sigma_0[1 - \exp(-r_\perp^2 Q_s^2/4)]$ , with the parameters determined by fitting small- $x$  HERA data.

In a similar way, the cross section for radiation of a virtual photon from a quark after scattering on a proton, has the following factorized form in impact parameter representation<sup>5</sup>,

$$\frac{d\sigma_{T,L}(qp \rightarrow \gamma^* X)}{d\ln \alpha} = \int d^2 r_\perp |\Psi_{\gamma^* q}^{T,L}(\alpha, r_\perp, \tilde{Q}^2)|^2 \sigma_{dip}(\tilde{x}, \alpha r_\perp), \quad (2)$$

where  $\Psi_{\gamma^* q}$  is the quark wavefunction representing the  $\gamma^* q$  fluctuation. Here,  $r_\perp$  is the photon-quark transverse separation,  $\alpha r_\perp$  is the  $q\bar{q}$  separation and  $\alpha$  is the fraction of the light-cone momentum of the initial quark taken away by the photon. Note the difference with the DIS case, where the dipole separation is just  $r_\perp$  and now the dipole cross section is evaluated for  $\alpha r_\perp$ . The scaling variable  $\tilde{x}$  is taken as  $x_2 = x_1 - x_F$ , which are the usual invariants in the fast proton system:  $x_{1,2}$  are the longitudinal momentum fractions of the projectile (target) parton and  $x_F$  is the Feynman variable. We stress that such identification is far from clear in the dipole picture: for instance, one can also choose  $\tilde{x} = \alpha x_2$ . In the rest frame, the quark carries momentum fraction  $x_1/\alpha$  of the parent hadron, where  $x_1$  is the proton's momentum fraction carried by the fóton. The hadronic differential cross section to Drell-Yan process is expressed in the factorized form<sup>5</sup>,

$$\frac{d\sigma^{DY}}{dM^2 dx_F} = \frac{\alpha_{em}}{6\pi M^2} \frac{1}{(x_1 + x_2)} \int_{x_1}^1 \frac{d\alpha}{\alpha} F_2^p\left(\frac{x_1}{\alpha}, \tilde{Q}^2\right) \frac{d\sigma(qp \rightarrow \gamma^* X)}{d\ln \alpha} \quad (3)$$

where the factor  $\alpha_{em}/(6\pi M^2)$  is due to the photon decay into a lepton pair, coming from electrodynamics. The dilepton invariant mass is  $M^2$ . Our input for  $\sigma_{dip}$  is constrained by the standard gluon distribution from the target

corrected by saturation effects in high energy limit, encoded in the Glauber-Mueller (GM) approach <sup>6</sup>. In Eq. (3), the structure of the projectile is described by the proton inclusive structure function  $F_2^p(x, \tilde{Q}^2)$ , in which was chosen  $\tilde{Q}^2 = M^2$ . Other possible identification relying on plausible arguments is  $\tilde{Q}^2 = (1 - x_1)M^2$  <sup>7</sup>. Our input for the dipole cross section is given by,

$$\sigma_{dip}^{GM}(\tilde{x}, r_\perp) = \frac{\pi^2 \alpha_s}{3} r^2 x G_N^{GM}(\tilde{x}, \frac{4}{r_\perp^2}), \quad (4)$$

$$x G^{GM}(\tilde{x}, Q^2) = \frac{2R^2}{\pi^2} \int_{\tilde{x}}^1 \frac{dx'}{x'} \int_{1/\tilde{Q}^2}^{1/Q_0^2} \frac{dr_\perp^2}{r_\perp^4} (\gamma_E + \ln[\kappa_G(x', r_\perp^2)] + E_1[\kappa_G(x', r_\perp^2)]) ,$$

where  $\gamma_E$  and  $E_1(x)$  are the Euler constant and the exponential integral. The packing factor is  $\kappa_G = (3\pi\alpha_s r_\perp^2 / 2R^2) x G^{\text{DGLAP}}$ . The saturation scale  $Q_s^2$  is defined through the relation  $\kappa_G(x, Q_s^2) = 1$ . The target transverse size is  $R$ , which was taken to be  $R^2 = 5 \text{ GeV}^{-2}$  (strong unitarity corrections) supported by previous studies<sup>3</sup>. The  $xG$  was parametrized by the GRV94 gluon density.

In a recent work<sup>8</sup>, we have calculated the DY cross section for the available small- $x_2$  data, and found that the dipole picture in that kinematical region ( $x_2 \geq 10^{-2}$ ) is being tested in its limit of applicability. As an improvement, we have introduced a reggeonic piece to account for the large  $x_2$  range in the phenomenological form  $\sigma_R(x, r_\perp) = N_R r_\perp^2 x^{0.4525} (1 - x)^3$ , which supplement Eq.(4). Towards smaller  $x_2$ , such contribution turns out to be negligible. In Ref.<sup>7</sup>, the procedure was to correct the saturation scale by a threshold factor  $Q_s^2 \rightarrow Q_s^2 (1 - x)^5$ , and the numeric equivalence between the dipole picture (using GBW model) and NLO DGLAP calculations is shown<sup>7</sup>, relying on an educated guess for the scales  $\tilde{x}$  and  $\tilde{Q}^2$ .

In order to address the color dipole picture at high energies<sup>8</sup> (small  $x_2$ ), the DY differential cross section for RHIC energies,  $\sqrt{s} = 500 \text{ GeV}$ , is shown in Fig. (1) for the same fixed  $x_F$ . In this case,  $x_2$  reaches values of order  $10^{-4}$  and unitarity effects are important. The solid lines are the GM estimates, Eq. (4), and the dot-dashed lines are the rest frame calculations with DGLAP gluon distribution (without parton saturation effects). The GM results underestimates those ones without parton saturation, showing important role of the unitarity effects. Moreover, we have obtained a result numerically equivalent to the LO Breit frame calculations at the RHIC energies, suggesting consistency between both approaches. From the plots one verifies that the deviations due to saturation effects are larger as  $M$  diminishes, corresponding to smaller  $x_2$  values. In absolute values, the corrections at RHIC energies reach up to  $\approx 20 \%$ , showing that saturation effects are important in a reliable description of the observables.

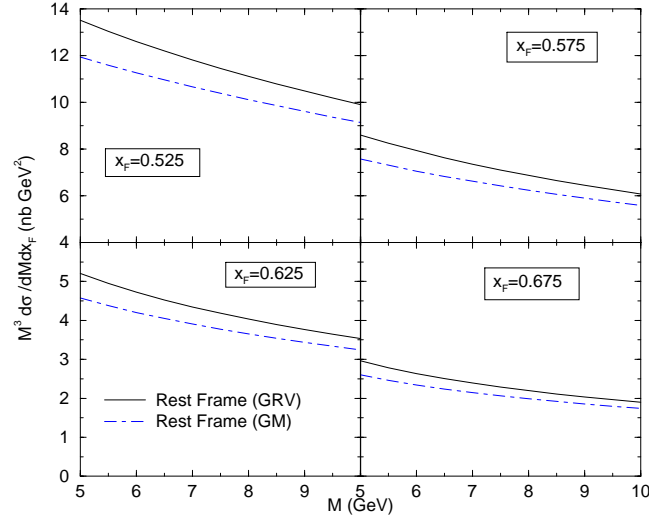


Figure 1. The DY differential cross section per nucleon versus  $M$  for the RHIC energies ( $\sqrt{s} = 500$  GeV) at fixed  $x_F$  in  $pd$  reaction. The solid line are GM estimates, whereas dot-dashed ones are without gluon saturation calculation.

### Acknowledgments

The authors enjoyed the lively scientific atmosphere of this meeting. This work is supported by CNPq, Brazil. MVTM thanks Jorg Raufeisen for discussions.

### References

1. M.B. Gay Ducati, *Braz. J. Phys.* **31**, 115 (2001).
2. S.J. Brodsky, A. Hebecker, E. Quack, *Phys. Rev. D* **55**, 2584 (1997);
3. M.B. Gay Ducati, M.V.T. Machado, *Phys. Rev. D* (to appear), [hep-ph/0111093].
4. K. Golec-Biernat, M. Wüsthoff, *Phys. Rev. D* **59**, 014017 (1999).
5. B.Z. Kopeliovich, J. Raufeisen, A.V. Tarasov, *Phys. Lett. B* **503**, 91 (2001).
6. A.L. Ayala, M.B. Gay Ducati, E.M. Levin, *Nucl. Phys. B* **511**, 355 (1998).
7. J. Raufeisen, J.-C. Peng, G.C. Nayak, [hep-ph/0204095].
8. M.A. Betemps, M.B. Gay Ducati, M.V.T. Machado, *Phys. Rev. D* (to appear), [hep-ph/0111473].